Special Feature: Analysis Techniques to Evaluate the Next Generation Electronic Materials

Research Report

Defect Detection in Semiconductor Materials by Luminescence Analysis

Keita Kataoka, Tetsuo Narita, Hiroko Iguchi, Masakazu Kanechika, Ken Hattori, Aishi Yamamoto and Tetsu Kachi

Report received on Dec. 27, 2018

ABSTRACT Luminescence methods such as cathodoluminescence (CL) and photoluminescence (PL) can sensitively detect crystal defects in semiconductor materials. In a luminescence spectrum, radiative defects show up as emission peaks at specific photon energies. The relative concentration of nonradiative defects can be evaluated by comparison with the total luminescence intensity, because nonradiative defects decrease the internal quantum efficiency. Furthermore, intentionally and unintentionally doped shallow impurities are also measurable in the near-band-edge region of the spectrum. In the present paper, we describe three different applications of CL and PL to defect analysis in semiconductor crystals, in order to highlight the importance of these techniques for characterizing electronic and optoelectronic devices.

KEYWORDS Cathodoluminescence, Photoluminescence, Crystal Defects, Gallium Nitride, Silicon

1. Introduction

Control of crystal defects in semiconductor materials for electronic and optoelectronic devices is key to improving device properties and reliability. Cathodoluminescence (CL) and photoluminescence (PL) can sensitively detect crystal defects in semiconductors. **Figure 1**(a) illustrates the experimental setup used for luminescence measurements. In the CL and PL techniques, electron-hole pairs are excited in the sample by, respectively, an incident electron beam and an optical beam with an energy greater than that of the bandgap. Upon recombination of the excited electron-hole pairs, the sample emits luminescence, which is spectrally analyzed using a monochromator and a detector.

Figure 1(b) shows the typical relaxation processes of the excited electron-hole pairs. These relaxation processes can be classified into radiative and nonradiative transitions. The former can be directly observed in the luminescence spectra. Not only intrinsic emission lines such as those due to free excitons but also extrinsic emission lines related to donor, acceptor, and defect states are measurable. On the other hand, defect states causing nonradiative transitions cannot be detected directly as emission peaks. However, nonradiative defects decrease the internal quantum efficiency (IQE) of the material. Thus, the relative density of nonradiative defects as a whole can be estimated by comparing the luminescence intensity for any emission line.[1]

In this paper, we review three applications of CL and PL measurements to defect analysis in semiconductor materials. In Secs. 2 and 3, we investigate defects induced in gallium nitride (GaN) by, respectively, dry

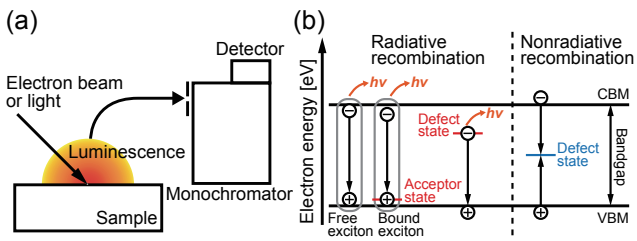

Fig. 1 (a) Experimental setup used for luminescence measurements. (b) Typical relaxation processes (radiative and nonradiative recombination) for excited electron-hole pairs in semiconductor materials are shown using a schematic energy band diagram. CBM and VBM stand for conduction band minimum and valence band maximum, respectively.

© Toyota Central R&D Labs., Inc. 2019

etching[2] and ion implantation.[3] Crystal defects are introduced unintentionally and transformed by various device fabrication processes, such as dry etching, ion implantation, and thermal annealing. Dry etching and ion implantation degrade the electrical properties of GaN-based electronic devices. Schottky diodes formed on a p-type GaN surface etched by inductively coupled plasma (ICP) showed an increase in series resistance owing to the compensation of acceptors.[4] In addition, p-n diodes fabricated by p-type doping through Mg-ion implantation and subsequent high-temperature annealing exhibited a high density of traps.[5] For both ICP etching and Mg-ion implantation, the suppression of defect generation and/or defect elimination are required for high-quality GaN-based devices. In the present study, defect formation by ICP etching or Mg-ion implantation, and the effect of thermal annealing were studied by CL analysis.

In Sec. 4, we examine the interaction between natively absorbed hydrogen and defects in silicon (Si) wafers.[6] Intrinsic defects exist originally in single-crystal wafers. In Si-based devices, these defects reduce the minority carrier lifetime, owing to recombination of carriers at defects.[7] Hydrogen termination of dangling bonds in vacancy-type defects is effective in increasing the minority carrier lifetime in Si.[8] The reactions of Si wafer defects with hydrogen are discussed on the basis of the thermal annealing dependence of the PL intensity.

2. Cathodoluminescence of ICP-etched GaN

2. 1 Experimental

Two-micron-thick n-type ([Si]: 5×10^{17} cm^{-3}) and p-type ([Mg]: 3×10^{19} cm^{-3}) GaN films were grown on c-plane sapphire substrates by metal-organic vapor phase epitaxy (MOVPE). The p-type samples were annealed at 850°C to activate the Mg acceptors. The samples were etched by ICP using a 1-Pa gas mixture of Cl_2 and BCl_3 with flow rates of 25 and 5 cm^3/min, respectively. The antenna power and bias power used during ICP etching were 300 and 60 W, respectively. After ICP etching, the samples were annealed at 900°C for 5 min in a N_2 atmosphere.

CL spectra were measured using a scanning electron microscope (JEOL, JSM-7000F) equipped with a CL system (HORIBA, MP-32MA-J). The acceleration voltage and beam current of the electron beam were 3 kV and 0.1 nA, respectively. Under these excitation conditions, the penetration depth of the electron beam was less than 100 nm. The CL spectra were obtained at room temperature.

2. 2 Results and Discussion

Figure 2(a) shows the CL spectra of the n-type GaN samples: a sample without ICP etching (w/o ICP sample), an ICP-etched sample (ICP 60 W sample), and a sample annealed at 900°C after ICP etching (ICP + 900°C sample). The peak at approximately 362 nm corresponds to band-edge luminescence. The peak intensities were significantly decreased by ICP etching. This decrease is thought to result from the decrease in the IQE caused by etching-induced nonradiative defects near the surface. The peak intensity slightly increased after annealing at 900°C, but did not fully recover to the level of the w/o ICP sample. These results indicate that the etching-induced nonradiative defects were partially repaired by annealing at 900°C, but their concentration was higher than that of the w/o ICP sample.

Figure 2(b) shows the CL spectra of the p-type GaN sample. The change in the band-edge luminescence intensity was similar to the n-type case described above. In p-type GaN, Mg-related peaks[9] were observed above 370 nm, in addition to the band-edge luminescence. After ICP etching, the Mg-related peaks disappeared completely, which indicates inactivation of the Mg acceptors near the surface. Upon annealing at 900°C, the Mg-related peaks reappeared as a result of the reactivation of the Mg acceptors.

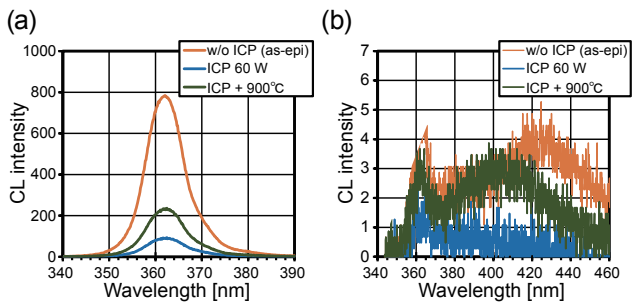

Fig. 2 Near-band-edge CL spectra for w/o ICP, ICP etching, and ICP etching + 900°C annealing samples of (a) p-type and (b) n-type GaN.[2]

© Toyota Central R&D Labs., Inc. 2019

2. 3 Summary

The etching damage induced by ICP and the effects of subsequent annealing were studied by CL. In both n-type and p-type GaN, nonradiative defects were introduced by ICP etching, which were partially eliminated by annealing at 900°C. In p-type GaN, the Mg acceptors were inactivated by ICP etching and reactivated by annealing at 900°C.

3. Cathodoluminescence of Mg-ion-implanted GaN

3. 1 Experimental

The p-n diode fabricated by implantation of Mg- and H-ions, which indicates superior rectification property at a forward voltage of about 3 V,[5] was measured by low temperature (LT)-CL and compared to the epitaxial sample. The N-polar n-type GaN(000$\bar{1}$) substrate was implanted with both Mg-ions and H-ions through a 30-nm-thick SiN film. The maximum concentrations of the Mg- and H-ions were 1.4×10^{19} and 2.1×10^{20} cm^{-3}, respectively. Under these conditions, a shallow junction with a depth of 0.1 µm was produced. After removal of the SiN film, the sample was annealed at 1230°C for 30 s in a N_2 atmosphere without any protective overlayers. The process conditions have been described in detail in a previous paper.[5] An epitaxial p-type GaN film with the same Mg concentration as the implanted sample was grown on an n-type GaN(0001) substrate by MOVPE. The sample was annealed at 850°C for 5 min in a N_2 atmosphere to remove the hydrogen in the film.

By using another set of samples, we studied the effects of the implantation depth and the annealing temperature. N-polar GaN(000$\bar{1}$) substrates were implanted with Mg- and H-ions through a 30-nm-thick SiN film. Junctions with depths of 0.1 µm ("shallow implantation") and 0.71 µm ("deep implantation") were formed using different implantation energies. In each case, the implantation depths of the Mg- and H-ions were almost the same. The shallow implantation conditions correspond to those for the p-n diode fabricated by ion implantation described at the beginning of this section. For deep implantation, box-shaped profiles of Mg- and H-ions with concentrations of 1.4×10^{19} and 2.1×10^{20} cm^{-3}, respectively, were produced by ions with multiple energies. After ion implantation, the samples were annealed in an N_2 atmosphere with no protective overlayer. To determine the effect of temperature, samples were annealed at 800 to 1230°C for 30 s.

LT-CL measurements were conducted at 10 K for all samples. The electron beam current was 1 nA, and the acceleration voltage was 3 or 5 kV, of which penetration depth was 80 or 160 nm, respectively.

3. 2 Results and Discussion

Figure 3(a) shows the CL spectra of the implanted p-n diode and the MOVPE-grown p-type GaN. For the MOVPE sample, the Mg-acceptor-related peaks were observed at 3.458 and 3.275 eV, which correspond to acceptor-bound excitons (ABEs) and donor-acceptor pairs (DAPs), respectively.[10] The peaks at 3.467 and 3.471 eV, observed as shoulders, were assigned to ABEs[11] and donor-bound excitons (DBEs),[12] respectively. The implanted p-n diode showed the same peaks as the MOVPE sample. The ABE and DAP peaks observed for the implanted p-n diode clearly demonstrate the formation of Mg acceptors.

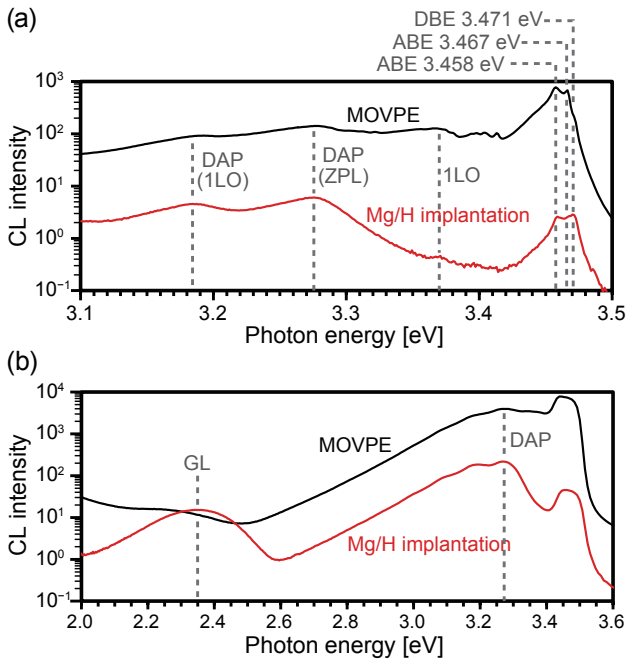

Fig. 3 CL spectra (5 kV) of the implanted p-n diode (red solid line) and the MOVPE-grown p-type GaN sample (black solid line) with the same Mg concentration, for (a) the NBE observed at high energy resolution, and (b) over a wide energy range.[3]

© Toyota Central R&D Labs., Inc. 2019

We found that the implanted Mg-ions were activated by the subsequent anneal at 1230°C. The DBE peaks observed for both samples are probably due to Si donors in the underlying n-type GaN layer.

The CL intensity for the implanted p-n diode, which is one to two orders of magnitude lower than that for the MOVPE sample, shows that a high concentration of nonradiative recombination centers (NRCs) exists in the implanted p-n diode even after the 1230°C anneal. Chichibu et al. reported that an increase in the NRC concentration causes the IQE to decrease even at low temperatures when all NRCs are located within the exciton volume.[13] By using their reasoning, the NRC concentration was estimated to be on the order of 10^{18} cm^{-3} for the implanted p-n diode. Figure 3(b) shows CL spectra over a wide energy range. The implanted p-n diode showed a characteristic green luminescence (GL) band around 2.35 eV, which is a common feature of GaN implanted by Mg-ions.[14,15] The GL band is thought to be due to nitrogen vacancy (V_N) complexes, and its appearance indicates that V_N-related point defects exist in the implanted p-n diode.

Figures 4(a) and (b) show the annealing temperature dependence of the CL spectra for the case of shallow and deep implantation, respectively. For both samples, ABE and DAP peaks were observed above 1000°C, and their intensity increased exponentially with increasing annealing temperature. Between 1000 and 1230°C, the lowest ABE and DAP intensities were found for the deep implantation sample, with the difference being about two orders of magnitude. These results indicate that the NRC concentration in the deep implantation samples is higher, presumably because of the higher implantation energy. The energy dissipation of Mg- and H-ions with higher kinetic energies should introduce more NRCs into the sample.

As shown in Fig. 4, the GL intensity at 2.0-2.6 eV and the near-band-edge (NBE) intensity at 2.85-4.0 eV both increased exponentially as the annealing temperature was increased above 1000°C. This is presumably the result of the decrease in NRC concentration. The defect analysis conducted by Uedono et al. through positron annihilation spectroscopy indicated that the concentration of vacancy clusters in the GaN sample implanted with Mg-ions decreased with increasing annealing temperature.[16] Their results are consistent with ours. However, there is a high concentration of residual NRCs (on the order of 10^{18} cm^{-3}) in the sample even after annealing at 1230°C. Therefore, a reduction in NRCs is expected to occur upon annealing above 1230°C.

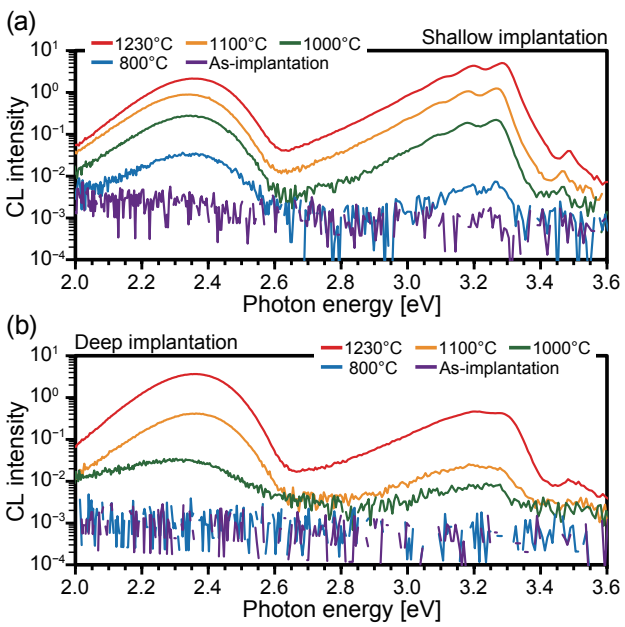

Fig. 4 Annealing-temperature-dependent CL spectra (3 kV) of (a) the shallow implantation and (b) deep implantation samples.[3]

3. 3 Summary

The implantation of GaN with Mg-ions and H-ions was investigated by LT-CL analysis. Comparing the CL spectra for the implanted p-n diode having superior rectification properties[5] with those for the epitaxial p-type GaN clearly revealed that Mg acceptors formed in the implanted p-n diode as a result of the 1230°C anneal. However, a high concentration of residual NRCs (~10^{18} cm^{-3}) was observed for the implanted p-n diode. V_N complexes were also identified in the CL spectra. Furthermore, a different set of samples was used to investigate the effects of implantation depth and annealing temperature. The deep implantation samples showed higher NRC concentrations than the shallow implantation samples, presumably owing to the higher implantation energies of the former. The NRC concentration decreased with increasing annealing temperature in the 1000-1230°C range. A further reduction in NRCs is expected to occur upon annealing above 1230°C.

© Toyota Central R&D Labs., Inc. 2019

4. Photoluminescence of Defects in Si Wafer

4. 1 Experimental

As-received samples were cut from a P-doped [(1.5-3.2) × 10^{12} cm^{-3}] FZ-Si(111) wafer. A flowchart of the experiments is shown in **Fig. 5**(a). Annealing under ultrahigh vacuum (UHV) was carried out, and in-situ PL measurements at a base pressure of less than 1 × 10^{-8} Pa were performed. The procedures for the 5-min anneal and the PL measurements at 82 K are shown in Fig. 5(b). For the PL measurements, the samples were excited by a continuous-wave diode laser with a wavelength of 655 nm. A 300-mm spectrometer and an InGaAs photomultiplier tube were used to obtain the PL spectra.

To forcibly introduce hydrogen into the Si wafer, ex-situ furnace annealing in H_2 was carried out. Ex-situ furnace annealing in N_2 was also performed for a comparison with the H_2-anneal. After the samples were exposed to air, they were annealed at 800°C for 60 min in a H_2 or N_2 atmosphere, and then cooled to room temperature while maintaining the H_2 or N_2 flow. The H_2 desorption from the samples was studied by temperature-programmed desorption (TPD) in another UHV system.[17] The experimental conditions have been described in detail elsewhere.[6]

4. 2 Results and Discussion

Figure 6(a) shows the normalized PL spectra of the as-received sample for different annealing temperatures in UHV. The peak at 1.10 eV was assigned to the transverse optical (TO) phonon-assisted decay of FEs.[18] The origin of the PL peaks was unchanged during annealing, as evidenced by the fact that the spectral shapes are almost the same. However, the TO-FE intensity (I^{TO}) changed upon annealing [circles in Fig. 6(b)]. Figure 6(b) shows that the I^{TO} for the as-received sample increased by a factor of 4.0 at 450°C, and decreased by a factor of 0.06 at 600°C. The changes in I^{TO} presumably result from the inactivation and activation of nonradiative defects in the sample.

The TPD curve corresponding to the desorption of H_2 molecules (mass-to-charge ratio, m/z = 2) for the as-received sample is shown in **Fig. 7**. There were two desorption peaks at approximately 420 and 600°C. Most of the H_2 must come from the bulk, because in UHV, physical adsorption of residual H_2 on the surface is negligible at 82 K.[19]

The remarkable I^{TO} drop by a factor of 0.06 at 600°C can be reasonably explained as the dissociation of

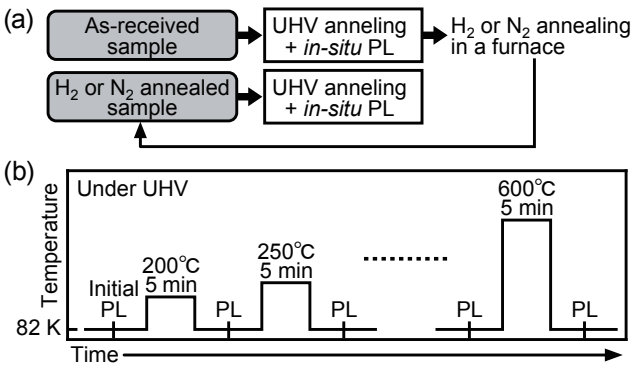

Fig. 5 (a) Flowchart of experiments. (b) Procedure for annealing and in-situ PL measurements in UHV.[6]

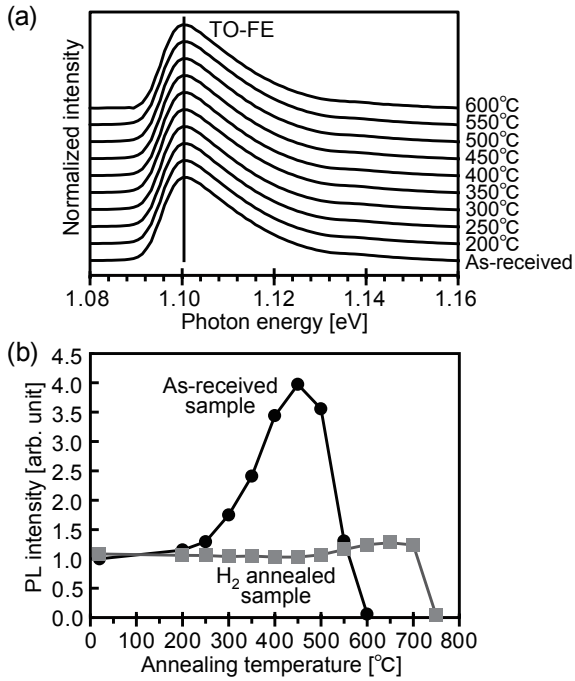

Fig. 6 (a) Normalized PL spectra at 82 K after UHV annealing at 200-600°C for an as-received sample. (b) PL intensity for TO-FE (I^{TO}) for as-received (circles) and H_2-annealed (squares) samples as a function of annealing temperature in UHV. The annealing duration was 5 min. All plotted data were normalized to the initial I^{TO} for the as-received sample.[6]

© Toyota Central R&D Labs., Inc. 2019

hydrogen from hydrogen-passivated defects. The activation of the inactivated defects leads to the observed decrease in I^{TO}. Natively absorbed hydrogen is presumably incorporated into the as-received wafer during melt growth in a hydrogen-containing environment.[20] Molecular hydrogen in the Si crystal migrates during melt growth at high temperature, and dissociates at defects.[21] The dissociated atomic hydrogen has the potential to passivate dangling bonds in defects such as vacancies.[22] Therefore, the as-received sample is expected to contain hydrogen-passivated defects. This natively absorbed hydrogen, which can be dissociated from the defects, is effused as H_2 at 600°C. Similar processes have been reported for Si-H bonds at defects at high temperature (T_h).[23,24] The TPD results shown in Fig. 7 indicate that the hydrogen content of the sample is negligible above T_h.

According to a previous TPD study, the diffusion and desorption of interstitial hydrogen molecules occurred at approximately 450°C below T_h.[24] This temperature, showing a maximum I^{TO} of 4.0 [Fig. 6(b)], is close to 420°C for the hydrogen desorption peak in Fig. 7, which implies that excess hydrogen diffuses and passivates active defects between 250-450°C accompanied by desorption. The hydrogen passivation of active defects increases I^{TO}.

Upon H_2 annealing, I^{TO} almost recovered to its initial value, a factor of 1.1 [squares in Fig. 6(b)]. On the other hand, the I^{TO} for the N_2-annealed sample was not fully restored, only a factor of 0.21. The I^{TO} recovery upon H_2-annealing confirms the inactivation of nonradiative defects by the hydrogen introduced.

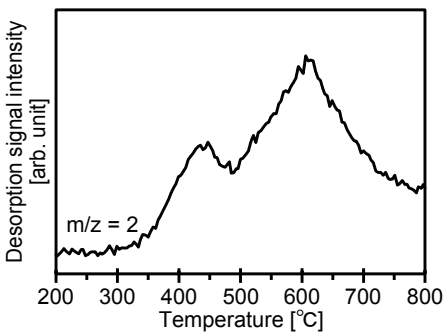

Fig. 7 Typical TPD curves (m/z = 2) for an as-received wafer. The heating rate was approximately 1.0°C/s.[6]

4. 3 Summary

Hydrogen passivation of defects in a high-quality FZ-Si wafer was investigated through PL measurements. The activation and inactivation of the defects corresponded to the drop and recovery of I^{TO}, which could be controlled reversibly by UHV annealing above 550°C and H_2 annealing at 800°C, respectively. The hydrogen absorbed during melt growth presumably passivated defects of a certain type in the commercial wafer. Another type of defect was likely passivated by excess hydrogen at 250-450°C. This inactivation process dramatically increased I^{TO} (to about 400% of its initial value) during annealing in UHV at 450°C.

5. Conclusion

Three applications of crystal defect analysis in semiconductor materials by CL or PL measurements were reviewed. In Sec. 2, the damage near the surface of the ICP-etched GaN was characterized by comparing the CL spectra. The changes in the nonradiative defect concentration were evaluated from the CL intensities of the band-edge luminescence. In Sec. 3, the thermal recovery process for GaN implanted with Mg- and H-ions was revealed by LT-CL spectra. Detailed analysis of the NBE peaks provided direct evidence of the formation of Mg acceptors upon subsequent annealing at 1230°C. Moreover, the relative concentrations of V_N complexes and other nonradiative defects for various annealing temperatures were discussed in terms of changes in the GL and NBE intensity, respectively. In Sec. 4, the interaction between nonradiative defects and the hydrogen in Si wafer was investigated by PL analysis. The PL intensity of the intrinsic FE peak reflected the activation and inactivation of vacancy-type defects, which correspond to hydrogen dissociation and hydrogen passivation of dangling bonds, respectively. CL and PL measurements, which can sensitively detect crystal defects in semiconductors, are essential for defect analysis for various semiconductor devices.

Acknowledgements

The work presented in Sec. 3 was supported by the Council for Science, Technology and Innovation, Cross-Ministerial Strategic Innovation Promotion (SIP) Program, funded by NEDO.

© Toyota Central R&D Labs., Inc. 2019

References

(1) Kataoka, K., Kimoto, Y., Horibuchi, K., Nonaka, T., Takahashi, N., Narita, T., Kanechika, M. and Dohmae, K., "Characterization of Ar Ion Etching Induced Damage for GaN", *Surf. Interface Anal.*, Vol. 44, No. 6 (2012), pp. 709-712.

(2) Kataoka, K., Kanechika, M., Narita, T., Kimoto, Y. and Uedono, A., "Positron Annihilation and Cathodoluminescence Study on Inductively Coupled Plasma Etched GaN", *Phys. Status Solidi B*, Vol. 252, No. 5 (2015), pp. 913-916.

(3) Kataoka, K., Narita, T., Iguchi, H., Uesugi, T. and Kachi, T., "Cathodoluminescence Study on Thermal Recovery Process of Mg-ion Implanted N-polar GaN", *Phys. Status Solidi B*, Vol. 255, No. 5 (2018), 1700379.

(4) Kato, M., Mikamo, K., Ichimura, M., Kanechika, M., Ishiguro, O. and Kachi, T., "Characterization of Plasma Etching Damage on *p*-type GaN Using Schottky Diodes", *J. Appl. Phys.*, Vol. 103, No. 9 (2008), 093701.

(5) Narita, T., Kachi, T., Kataoka, K. and Uesugi, T., "P-type Doping of GaN($000\bar{1}$) by Magnesium Ion Implantation", *Appl. Phys. Express*, Vol. 10, No. 1 (2017), 016501.

(6) Kataoka, K., Hattori, K., Yamamoto, A., Harroti, A. N., Hatayama, T., Kimoto, Y., Endo, K., Fuyuki, T. and Daimon, H., "Enhancements of Photoluminescence Intensity in High-quality Floating-zone Si by Thermal Annealing in Vacuum", *Jpn. J. Appl. Phys.*, Vol. 55, No. 11 (2016), 110308.

(7) Ross, B., "Survey of Literature on Minority Carrier Lifetimes in Silicon and Related Topics", *Lifetime Factors in Silicon* (1980), pp. 14-28, American Society for Testing and Materials.

(8) Pankove, J. I., "Chapter 1 Introduction", *Semiconductors and Semimetals*, Vol. 21, Part B (1984), pp. 1-10, Elsevier.

(9) Reshchikov, M. A. and Morkoç, H., "Luminescence Properties of Defects in GaN", *J. Appl. Phys.*, Vol. 97, No. 6 (2005), 061301.

(10) Pozina, G., Paskov, P. P., Bergman, J. P., Hemmingsson, C., Hultman, L., Monemar, B., Amano, H., Akasaki, I. and Usui, A., "Metastable Behavior of the UV Luminescence in Mg-doped GaN Layers Grown on Quasibulk GaN Templates", *Appl. Phys. Lett.*, Vol. 91, No. 22 (2007), 221901.

(11) Monemar, B., Paskov, P. P., Pozina, G., Hemmingsson, C., Bergman, J. P., Kawashima, T., Amano, H., Akasaki, I., Paskova, T., Figge, S., Hommel, D. and Usui, A., "Evidence for Two Mg Related Acceptors in GaN", *Phys. Rev. Lett.*, Vol. 102, No. 23 (2009), 235501.

(12) Kornitzer, K., Ebner, T., Thonke, K., Sauer, R., Kirchner, C., Schwegler, V., Kamp, M., Leszczynski, M., Grzegory, I. and Porowski, S., "Photoluminescence and Reflectance Spectroscopy of Excitonic Transitions in High-quality Homoepitaxial GaN Films", *Phys. Rev. B*, Vol. 60, No. 3 (1999), pp. 1471-1473.

(13) Chichibu, S. F., Kojima, K., Uedono, A. and Sato, Y., "Defect-resistant Radiative Performance of *m*-plane Immiscible $Al_{1-x}In_xN$ Epitaxial Nanostructures for Deep-ultraviolet and Visible Polarized Light Emitters", *Adv. Mater.*, Vol. 29, No. 5 (2017), 1603644.

(14) Kojima, K., Takashima, S., Edo, M., Ueno, K., Shimizu, M., Takahashi, T., Ishibashi, S., Uedono, A. and Chichibu, S. F., "Nitrogen Vacancies as a Common Element of the Green Luminescence and Nonradiative Recombination Centers in Mg-implanted GaN Layers Formed on a GaN Substrate", *Appl. Phys. Express*, Vol. 10, No. 6 (2017), 061002.

(15) Tadjer, M. J., Feigelson, B. N., Greenlee, J. D., Freitas Jr., J. A., Anderson, T. J., Hite, J. K., Ruppalt, L., Eddy Jr., C. R., Hobart, K. D. and Kub, F. J., "Selective p-type Doping of GaN:Si by Mg-ion Implantation and Multicycle Rapid Thermal Annealing", *ECS J. Solid State Sci. Technol.*, Vol. 5, No. 2 (2016), pp. 124-127.

(16) Uedono, A., Takashima, S., Edo, M., Ueno, K., Matsuyama, H., Kudo, H., Naramoto, H. and Ishibashi, S., "Vacancy-type Defects and Their Annealing Behaviors in Mg-implanted GaN Studied by a Monoenergetic Positron Beam", *Phys. Status Solidi B*, Vol. 252, No. 12 (2015), pp. 2794-2801.

(17) Hattori, A. N., Hattori, K., Moriwaki, Y., Yamamoto, A., Sadakuni, S., Murata, J., Arima, K., Sano, Y., Yamauchi, K., Daimon, H. and Endo, K., "Enhancement of Photoluminescence Efficiency from GaN(0001) by Surface Treatments", *Jpn. J. Appl. Phys.*, Vol. 53, No. 2 (2014), 021001.

(18) Dean, P. J., Haynes, J. R. and Flood, W. F., "New Radiative Recombination Processes Involving Neutral Donors and Acceptors in Silicon and Germanium", *Phys. Rev.*, Vol. 161, No. 3 (1967), pp. 711-729.

(19) Govers, T. R., Mattera, L. and Scoles, G., "Molecular Beam Experiments on the Sticking and Accommodation of Molecular Hydrogen on a Low-temperature Substrate", *J. Chem. Phys.*, Vol. 72, No. 10 (1980), pp. 5446-5455.

(20) Hara, A., Koizuka, M., Aoki, M., Fukuda, T., Yamada-Kaneta, H. and Mori, H., "Influence of Grown-in Hydrogen on Thermal Donor Formation and Oxygen Precipitation in Czochralski Silicon Crystals", *Jpn. J. Appl. Phys.*, Vol. 33, No. 10 (1994), pp. 5577-5584.

(21) Estreicher, S. K., Hastings, J. L. and Fedders, P. A., "Defect-induced Dissociation of H_2 in Silicon", *Phys. Rev. B*, Vol. 57, No. 20 (1998), pp. R12663-R12665.

© Toyota Central R&D Labs., Inc. 2019

(22) Pearton, S. J., Corbett, J. W. and Shi, T. S., "Hydrogen in Crystalline Semiconductors", *Appl. Phys. A*, Vol. 43, No. 3 (1987), pp. 153-195.
(23) Stutzmann, M. and Brandt, M. S., "Deuterium Effusion Measurements in Doped Crystalline Silicon", *J. Appl. Phys.*, Vol. 68, No. 3 (1990), pp. 1406-1409.
(24) Stutzmann, M., Chevrier, J.-B., Herrero, C. P. and Breitschwerdt, A., "A Comparison of Hydrogen Incorporation and Effusion in Doped Crystalline Silicon, Germanium, and Gallium Arsenide", *Appl. Phys. A*, Vol. 53, No. 1 (1991), pp. 47-53.

Fig. 2
Reprinted from Phys. Status Solidi B, Vol. 252, No. 5 (2015), pp. 913-916, Kataoka, K., Kanechika, M., Narita, T., Kimoto, Y. and Uedono, A., Positron Annihilation and Cathodoluminescence Study on Inductively Coupled Plasma Etched GaN, © 2015 Willey-VCH, with permission from Wiley-VCH Verlag.

Figs. 3-4
Reprinted from Phys. Status Solidi B, Vol. 255, No. 5 (2018), 1700379, Kataoka, K., Narita, T., Iguchi, H., Uesugi, T. and Kachi, T., Cathodoluminescence Study on Thermal Recovery Process of Mg-ion Implanted N-polar GaN, © 2018 Willey-VCH, with permission from Wiley-VCH Verlag.

Figs. 5-7
Reprinted from Jpn. J. Appl. Phys., Vol. 55, No. 11 (2016), 110308, Kataoka, K., Hattori, K., Yamamoto, A., Harroti, A. N., Hatayama, T., Kimoto, Y., Endo, K., Fuyuki, T. and Daimon, H., Enhancements of Photoluminescence Intensity in High-quality Floating-zone Si by Thermal Annealing in Vacuum, © 2016 The Japan Society of Applied Physics.

Keita Kataoka

Research Fields:
- Semiconductor Physics
- Surface and Interface Analysis

Academic Degree: Dr.Sci.
Academic Society:
- The Japan Society of Applied Physics

Tetsuo Narita

Research Field:
- III-Nitride Semiconductor: Growth, Power Device and Physics

Academic Degree: Dr.Eng.
Academic Society:
- The Japan Society of Applied Physics

Awards:
- Best Young Scientist Award, The 6th International Symposium on Growth of III-Nitrides, The Chemical Society of Japan, 2015
- Young Scientist Presentation Award, JSAP Fall Meeting, 2004

Hiroko Iguchi

Research Field:
- Research on Process Technology for Power Device

Academic Society:
- The Japan Society of Applied Physics

Masakazu Kanechika

Research Field:
- Process and Design of Power Device and Compound Semiconductor

Academic Degree: Dr.Eng.
Academic Societies:
- The Japan Society of Applied Physics
- IEEE Electron Devices Society

Award:
- JJAP Outstanding Paper Award, The Japan Society of Applied Physics, 2008

© Toyota Central R&D Labs., Inc. 2019

Ken Hattori*
Research Field:
- Surface Science

Academic Degree: Dr.Sci.
Academic Societies:
- The Physical Society of Japan
- The Japan Society of Vacuum and Surface Science

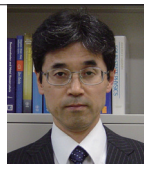

Aishi Yamamoto**
Research Field:
- Optical Properties of Semiconductor Materials

Academic Degree: Ph.D.
Academic Societies:
- The Physical Society of Japan
- The Japan Society of Applied Physics

Tetsu Kachi
Research Field:
- Power Electronics and Power Devices

Academic Degree: Dr.Eng.
Academic Societies:
- The Japan Society of Applied Physics
- The Institute of Electronics, Information and Communication Engineers

Award:
- JJAP Outstanding Paper Award, The Japan Society of Applied Physics, 2008

Present Affiliation: Nagoya University

*Nara Institute of Science and Technology
**Hiroshima Institute of Technology

© Toyota Central R&D Labs., Inc. 2019